Narrow band reduction of the mosaic of M83

Document number:	M2600-0000-032
Revision:	2
Classification:	Public
Prepared by:	S. Passmoor
Date:	14 March 2022

Organisation	:	NRF (National Research Foundation)
Facility	:	SARAO (South African Radio Astronomy Observatory)
Project	:	MeerKAT
Document Type	:	Report
Function/Discipline	:	Science commissioning

Document Approval

	Name	Designation	Affiliation	Signature/Date
Submitted by	S. Passmoor	Commissioning Scientist	SARAO	SPassmoor
Reviewed by	S. Goedhart	Manager: Commissioning	SARAO	SGoedhart Sharmila Goedhart (Mar 14, 2022 15:40 GMT+2)

Document History

Revision	Date of Issue	Person Responsible	Comments
A	16 March 2020	S. Passmoor	First draft
1	25 March 2020	S. Passmoor	Accepted and Signed
2	14 May 2020	S. Passmoor	Updated with results after the release of a new correlator version that fixes an off by 1 channel labelling bug

Document Software

	Package	Version	Filename
Stylesheet	katscidoc	3.0	katscidoc.sty
Word processor	LaTeX:TeXShop	4.44	
Radio interferometry imaging	CASA	5.6.2-2 PIPELINE variant	
Source Finding Application	SoFiA	2.1.0 (19-Nov-2019)	
Source Finding Application	SoFiA	2.1.1 (15-Apr-2020)	

Organisation Details

Name	SARAO Johannesburg Office (Rosebank, Gauteng)	SARAO, Cape Town Office (Observatory, Cape Town)	SARAO HartRAO (Hartebeesthoek, Gauteng)	SARAO, Karoo Astronomy Reserve (Carnarvon, Northen Cape)
Physical / Postal Address	1st Floor, 17 Baker Street Rosebank, Gauteng 2196, South Africa	2 Fir Street (North Entrance) Black River Park, Observatory Cape Town, 7925	PO Box 443 Krugersdorp 1740, South Africa	Posbus 69 Carnarvon 8925, South Africa
Tel.	+27 11 268 3400	+27 21 506 7300	+27 12 301 3100	+27 21 506 7300
Fax	+27 11 442 2454	+27 21 506 7375	+27 12 301 3300	+27 86 538 6836
Website	http://www.ska.ac.za	http:www.ska.ac.za	http:www.ska.ac.za	http:www.ska.ac.za

Contents

List of Figures

List of Tables

List of Abbreviations

ATCA	Australian Telescope Compact Array
CAM	Control and Monitoring
CASA	Common Astronomy Software Applications
LADUMA	Looking At the Distant Universe with the MeerKAT Array
LSRK	Local Standard of Rest Kinematic
LSP	Large Survey Project
LVHIS	Local Volume HI Survey
MHONGOOSE	MeerKAT HI Observations of Nearby Galactic Objects : Observing Southern Emitters
rms	Root mean square
SKA	Square Kilometre Array
SoFiA	Source Finding Application
THINGS	The HI nearby Galaxy Survey
T_{sys}/η	System temperature over aperture efficiency
VLA	Very Large Array

1 Summary

M83, a nearby galaxy, was observed on the 4th of March 2020 and on the 10th of April 2020 with the new 107 MHz narrow band correlator mode. The two observations differ in that in the second observation a correlator bug has been fixed. The bug was causing an offset of channel numbering by one. The data were reduced with a standard reduction procedure and the detected neutral hydrogen emission was extracted from the data product. The image noise level was 15% and 13% higher, respectively, than the theoretically predicted level. This difference is not a serious problem as it is likely to be alleviated by using more sophisticated calibration procedures, such as self-calibration, than those that were used in the standard reduction procedure in this report. The final image produced for the 4th of March observation has a resolution of 24.46 by 22.00 arc seconds with 4096 by 4096 pixels and the final image for the 10th of April observation has a resolution of 22.73 by 19.47 arc seconds. A total of 640 channels were imaged, from 1417.12 MHz to 1418.69 MHz.

2 Introduction

2.1 Background

M83 (NGC 5236) is a spiral galaxy with active star formation near the centre of a small group of galaxies. The source has an optical extent of 12.9' x 11.5' but the HI extent is around a degree in scale. The galaxy has a HI integrated flux of 1630.3 Jy km/s, a peak flux of 7.710 Jy (Barnes et al. 2001), and a distance of $D_{cepheid} = 4.5 \pm 0.3$ Mpc. This makes the source one of the brightest extragalactic HI sources in the southern sky.

There are multiple HI observations of M83 with comparable baseline distributions: with the Australia Telescope Compact Array (ATCA) as part of "The Local Volume HI Survey" (LVHIS) (Park et al. 2001), and with the Very Large Array (VLA) as part of "The HI nearby Galaxy Survey" (THINGS) (Walter et al. 2008). The galaxy has a recessional velocity of 513 km/s putting it outside of the Galactic HI and associated high velocity clouds of our galaxy. There is also a spectrum from the HIPASS survey (Barnes et al. 2001).

2.2 LVHIS ACTA data comparison

LVHIS presented the 9-point mosaic of M83, done with ATCA in Koribalski (2018). This provides a comparable dataset for us examine the accuracy of our data. The beam in the LVHIS mosaic is 85.8" x 60.8" and was done with natural weighting. A plot of the LVHIS mosaic of M83 is shown in Figure 1. In the centre plot we have matched the contours to be the same in both the LVHIS images on the top and the MeerKAT images in the middle and bottom rows.

2.3 Commissioning task and testing

The choice of this field and type of observation for science commissioning was done on the basis that this would provide a test of the sort of observation that the accepted Large Survey Projects such as the MHONGOOSE Project or the Fornax Project would perform. (The LADUMA LSP will do a very long integration on a piece of sky and seeks to discover faint and unknown galaxies.) This is primarily a test of the narrow spectral line correlator mode, for imaging neutral hydrogen. We can expect to be able to reproduce the THINGS and LVHIS observations with the MeerKAT radio telescope. The antennas used in this observation are shown in Figure 2; in the second observation 3 additional antennas were available which provided additional intermediate baselines.

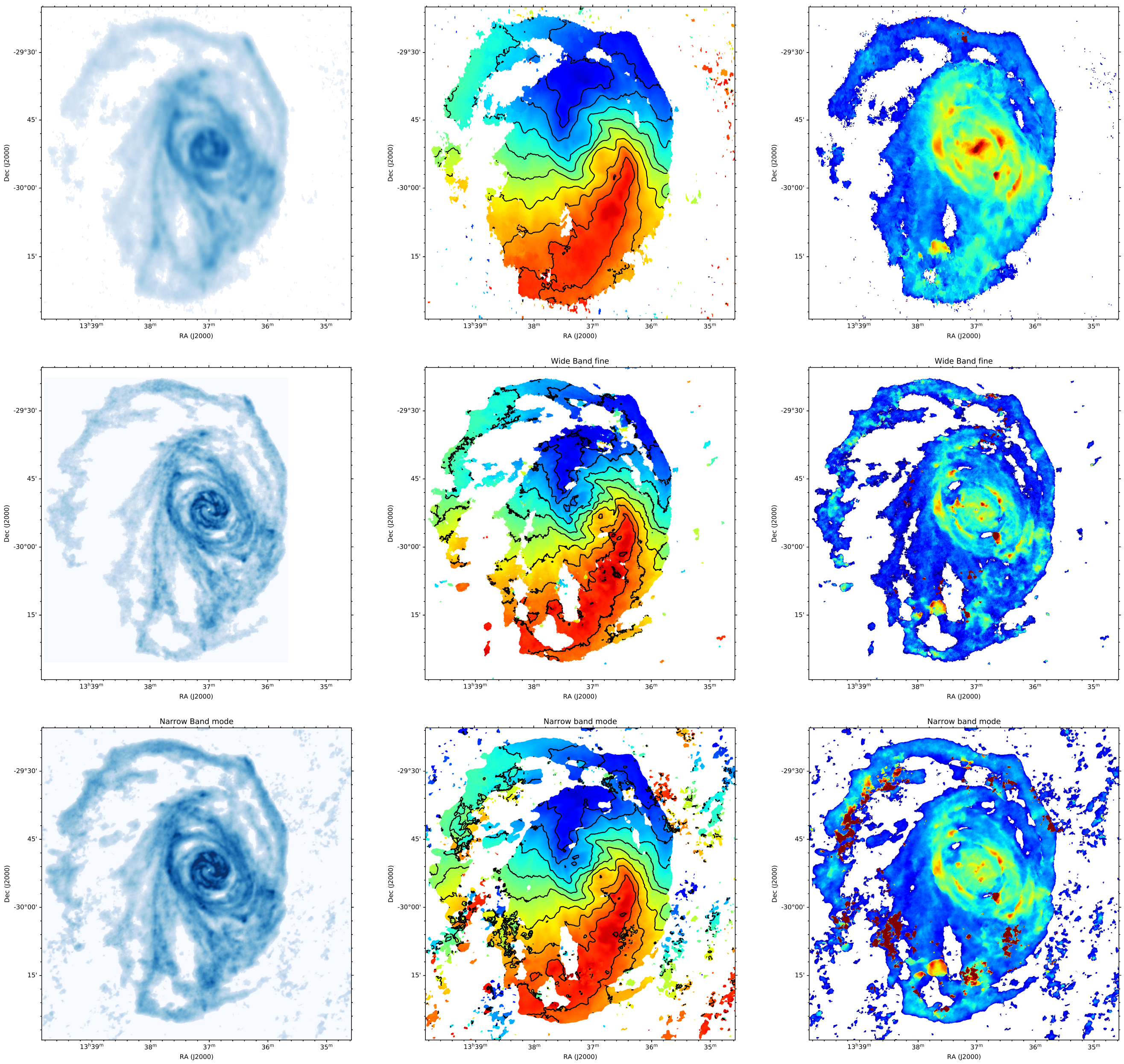

Figure 1: Images of M83 from the Local Volume *HI* Survey (LVHIS) Koribalski (2018) (top), the MeerKAT wide band fine (32K channels acrosss the full band) observation on the 8th of December 2019 (middle) and the MeerKAT Narrow band observation on the 10th of April 2020 (bottom) with the same colour scales. The graphs left to right are the integrated value of the spectrum, the intensity weighted coordinate, and the intensity weighted dispersion of the coordinate. The contours levels in the middle plot are: 649, 617.5, 586, 554.6, 523.1, 491.7, 460.2, 428.7, 397.3, 365.8 $km.s^{-1}$

Table 1: Observation and Correlator values of the two observations that are used in this report.

Parameter	4th March	10th April
Filename	1583350276_sdp_l0.full.rdb	1586545113_sdp_l0.full.rdb
Observed from	2020-03-04 19:31:29 UTC	2020-04-10 18:58:45 UTC
Observed to	2020-03-05 06:30:25 UTC	2020-04-11 05:55:39 UTC
Dump period	8.153 seconds	8.153 seconds
Correlator mode	c856M4k_n107M	c856M4k_n107M
Centre Frequency	1400 MHz	1400 MHz
Correlator Band-width	107 MHz	107 MHz
Channel Width	3.265 kHz	3.265 kHz
Channel Width	0.69 $km.s^{-1}$	0.69 $km.s^{-1}$
Number of dumps	4849	4834
Number of channels	32768	32768
Number of correlation products	6612	7320
Number of Antennas	57	60
Size of Observation	8404.753 GB	9275.934 GB
Correlator version	2020-03-03-16h33-devel-a22491...'	0.1.dev1606+devel.596db29.dirty

3 The Observation

3.1 Observational setup

The observation has 7 pointings of the mosaic centred on M83 with a separation of 0.707 degrees shown in Figure 3. The centre pointing on M83 is labeled $M83_4$. The complex gain calibrator for the observation was PKS1313-33, which is 5.8 degrees from M83 but only has a flux of 0.695 Jy. Two Flux and Bandpass calibrators were included, PKS0408-65 and PKS1934-638, to ensure that there will always be one up above 20 degrees elevation. The observation was run using a generic script that loops through all the targets and complex gain calibrator, and periodically visits any/all available bandpass/flux calibrators. We chose to observe the bandpass calibrator for 600 seconds every hour during the observation, with the seven mosaic targets observed for 100 seconds each and the complex gain calibrator was observed for 120 seconds. This means that the complex gain calibrator would be observed every ≈ 16 minutes. 17% of observing time was spent slewing between all the calibrators and target. This is not an optimal setup for scientific observations but was chosen in order to have additional checks on gain and system stability.

3.2 Observation data

The first M83 Narrow-band Commissioning test observation was observed from 2020-03-04 19:31 UTC to 2020-03-05 06:30 UTC with 57 antennas in the c856M4k_n107M correlator mode. The band had a centre frequency of 1400 MHz and a band width of 107 MHz giving a channel width of 3.265kHz or 0.69 $km.s^{-1}$. The second Narrow-band Commissioning test observation, completed after the fix of the channel labelling error had been corrected was observed from 2020-04-10 18:58:45 UTC to 2020-04-11 05:55:39 UTC with the same centre frequency. A comparison of the results of the two data sets can be seen in Figure 4. It should be noted that a lower noise threshold was obtained in second data set which can be seen in the the appearance of the low level emission that is seen outside the galaxy.

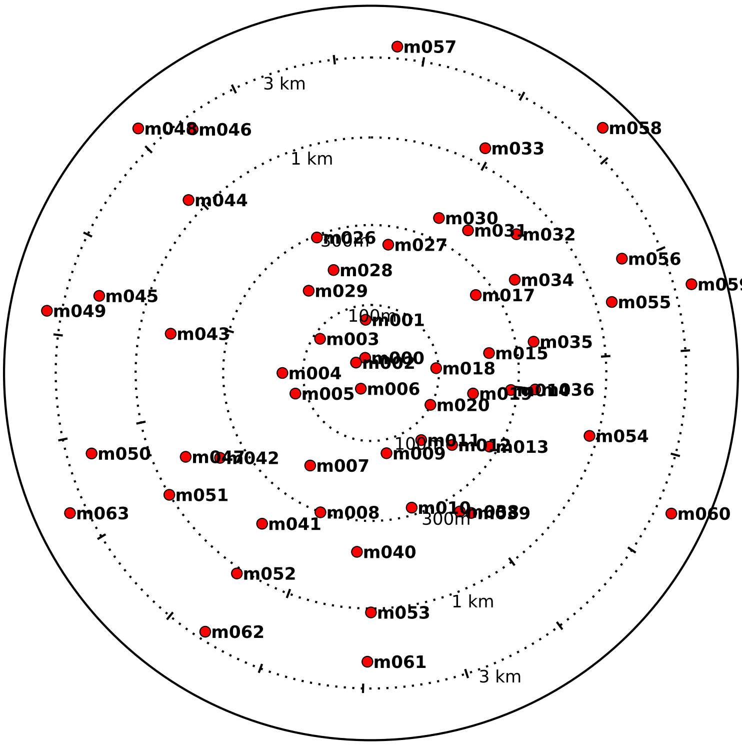

Figure 2: A log radial plot of 57 antennas that were used in the first observation. The MeerKAT antenna distribution consists of two co-centric Gaussian distributions, one that has a spread to $1Km$ and other out to $4Km$.

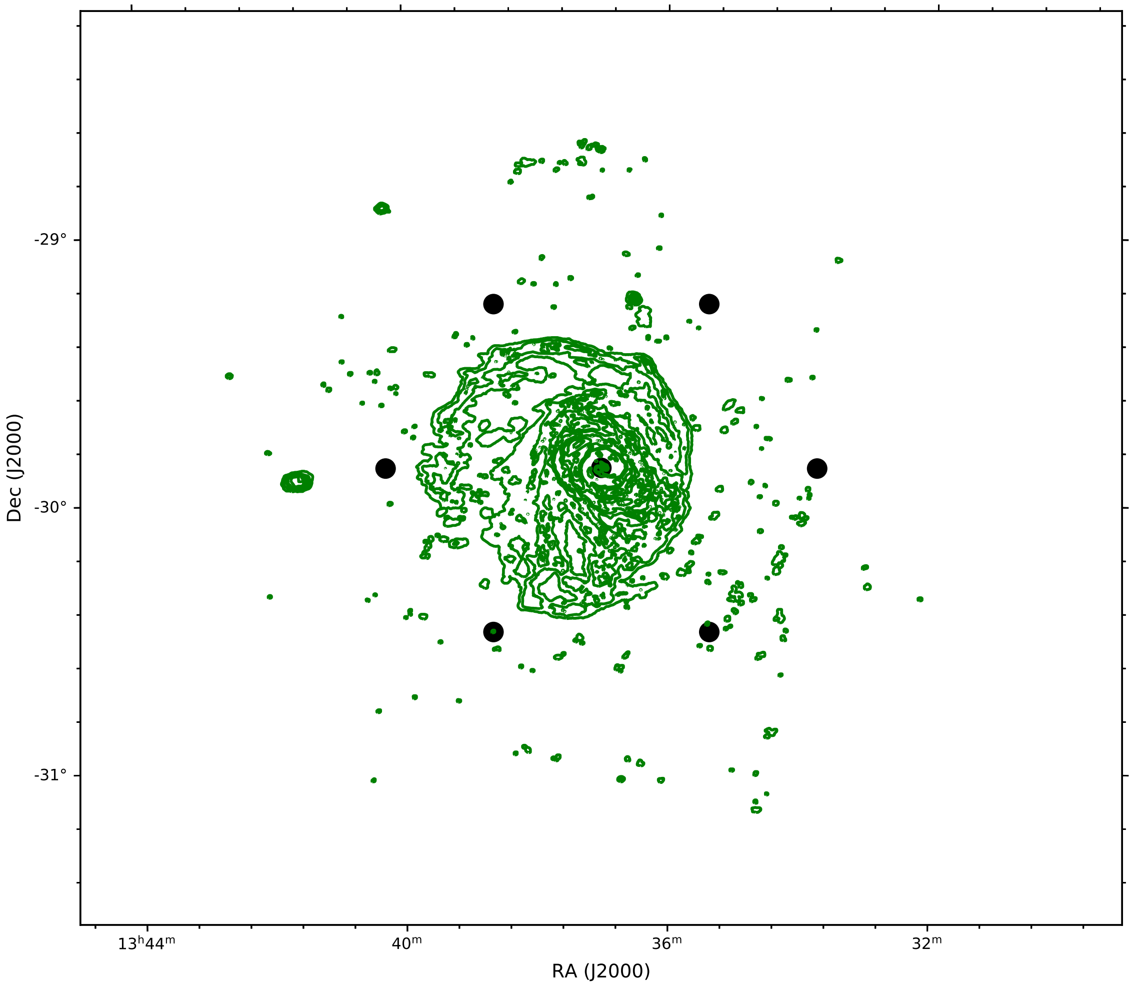

Figure 3: HI contours (green), with the pointing centre of each of the fields in the mosaic overlaid in grey. Each pointing was separated by $1/\sqrt{2}$ degrees to ensure uniform response of the telescope over the imaged area (assuming the telescope has a 1 degree FWHM beam).

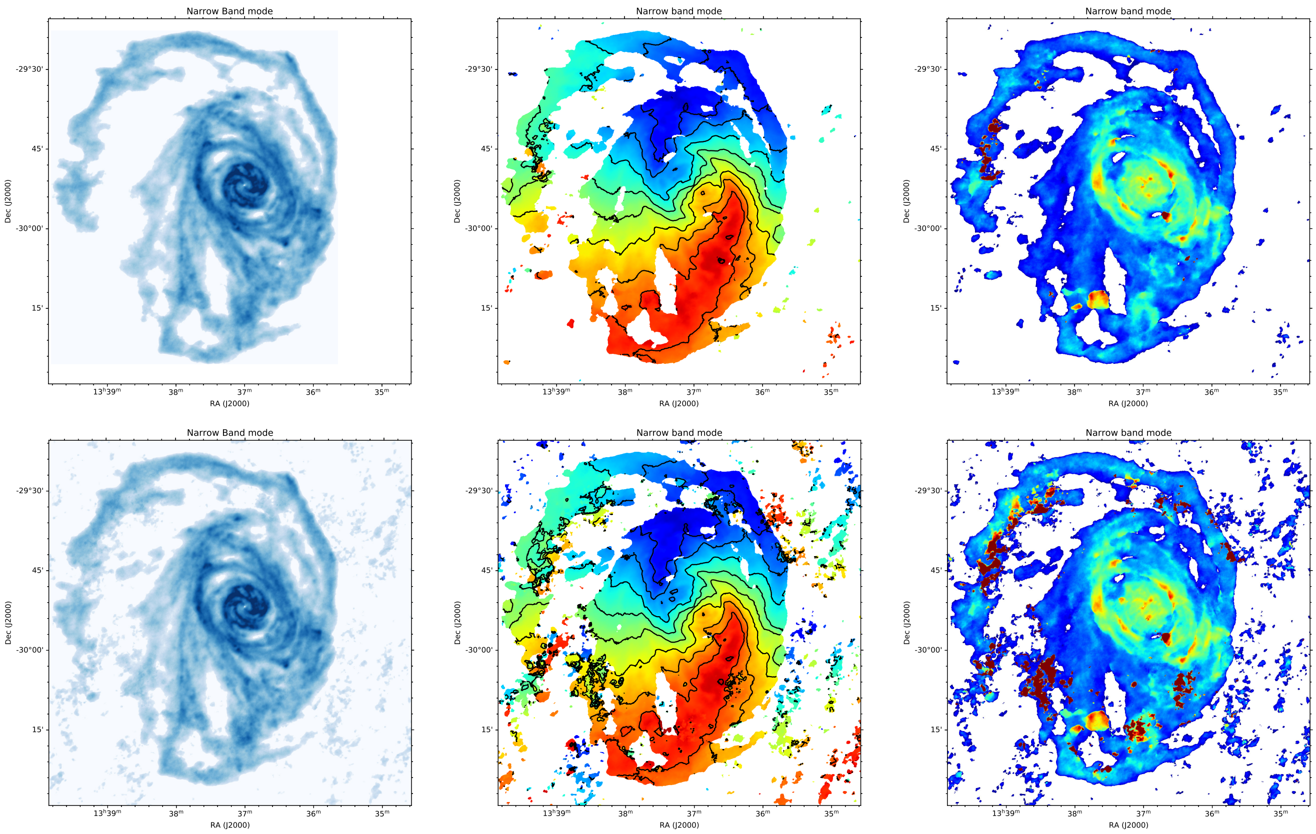

Figure 4: A comparison of the two narrow band images of M83 from the MeerKAT Narrow band observation on the 4th of March 2020 (top) and the MeerKAT Narrow band observation on the 10th of April 2020 (bottom) with the same colour scales. The graphs left to right are the integrated value of the spectrum, the intensity weighted coordinate, and the intensity weighted dispersion of the coordinate. The contours levels in the middle plot are: 649, 617.5, 586, 554.6, 523.1, 491.7, 460.2, 428.7, 397.3, 365.8 $km.s^{-1}$. The observation on the 10th of April 2020 (bottom) was able to get closer to the thermal noise.

Table 2: The theoretical noise per channel, calculated per field based on the number of un-flagged visibilities for the 4th of March observation . The mean measured system temperature across the frequency range of the image is $T_{sys}/\eta = 19.7$K.

Source	Time on source (minutes)	Theoretical RMS $T_{sys} = 19.73$K
J0408-6545	19.8	2.428 mJy
PKS1313-333	66.7	1.324 mJy
J1311-2216	32.3	1.902 mJy
J1939-6342	29.8	1.983 mJy
$M83_0$	55.2	1.456 mJy
$M83_1$	53.5	1.478 mJy
$M83_2$	53.3	1.482 mJy
$M83_3$	53.5	1.478 mJy
$M83_4$	53.1	1.484 mJy
$M83_5$	53.9	1.473 mJy
$M83_6$	53.1	1.484 mJy
J1331+3030	19.8	2.428 mJy

4 Data inspection

4.1 Flagging data

A subset of data from 1410 MHz to 1422 MHz (channels 19446,23121) was exported to measurement set format and the flagging was done as detailed below. There was no data flagged for antenna shadowing. Galactic HI was flagged from the flux calibrator PKS1934-638 in channels 1420.1833 MHz to 1420.2976 and in channels 1420.4086 MHz to 1420.5425 MHz. In the gain calibrator PKS1313-333, Galactic HI was flagged in the range 1420.3956 MHz to 1420.5947 MHz. In the first data set Antenna M003 was flagged due to poor data quality, while in the second data set Antenna M030 was flagged due to poor data quality.

4.2 Theoretical sensitivity

After removing slews and flagging as detailed in sections above we calculate the accumulated time on target for the two narrow band observations that were conducted, which is detailed in Table 2 and in Table 3 . Using the system temperature $T_{sys}/\eta = 19.73$K we can calculate the theoretical sensitivity. The two observations are of similar overall length but due to scheduling differences there is a small difference in the amount of time on the target fields. The 10th of April observation has less time on target but more antennas in the observation this in general seems to cancel out so that the sensitivities are very similar.

5 Reducing the data

The reduction process and tasks were performed using the CASA python system. The parameters for the observation and reduction were chosen to ensure that any array or antenna problems would not be unintentionally calibrated out or obscured.

PKS1934-638 was used as the flux, bandpass and delay calibrator in this observation. Delay calibration was done on each of the scans on PKS1934-638 and the delays were found to only have a scatter of ± 0.1

Table 3: The theoretical noise per channel, calculated per field based on the number of un-flagged visibilities for the 10th of April observation . The mean system temperature across the frequency range $T_{sys}/\eta = 19.73$K.

Source	Time on source (minutes)	Theoretical RMS $T_{sys} = 19.73$K
J0408-6545	29.8	1.883 mJy
PKS1313-333	55.2	1.383 mJy
J1311-2216	26.4	2.000 mJy
J1939-6342	89.6	1.085 mJy
$M83_0$	48.0	1.483 mJy
$M83_1$	46.9	1.500 mJy
$M83_2$	47.4	1.491 mJy
$M83_3$	49.2	1.464 mJy
$M83_4$	46.7	1.502 mJy
$M83_5$	48.0	1.483 mJy
$M83_6$	47.3	1.494 mJy
J1331+3030	19.8	2.306 mJy

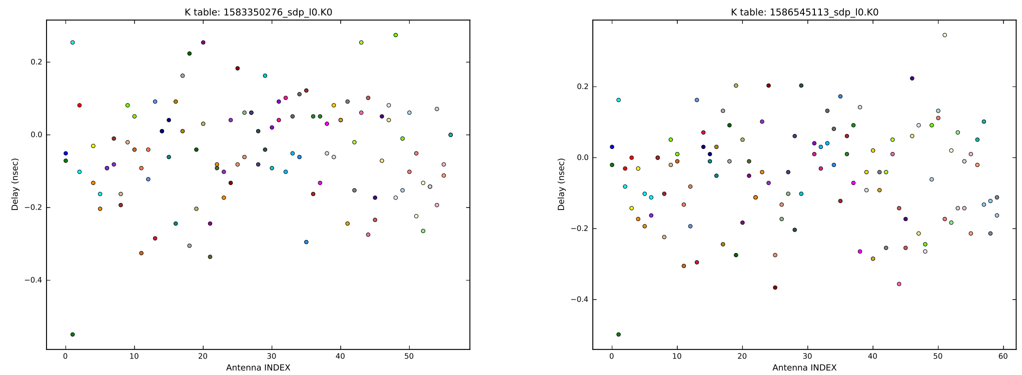

Figure 5: The Delay calibration was done on the combined scans of PKS1934-638 for both of the narrow band datasets, the 4th of March (left) and the 10th of April (right). The delays were found to only have a scatter of ± 0.3 nanoseconds and no offset that would indicate that delays from the subarray build's delay calibrations not being applied. This was a concern as there may have been issues where only one of the two correlators that are operating when running may get the calibration values to be set.

nanoseconds over the observation; following this all the combined scans from PKS1934-638 were used to generate a single delay calibration for the observation in Figure 5.

An initial complex gain calibration was done on PKS1934-638 and was used to produce a bandpass and flux calibration from all the combined PKS1934-638 scans.

The complex gain table was then discarded and recalculated using PKS1313-333 together with the delay and bandpass calibration. The flux scaling for the complex gain was calculated and applied to the seven mosaic fields and the seven fields were then split out. Continuum emission was fitted over 1411.11 MHz to 1415.55 MHz and 1419.74 MHz to 1425.48 MHz with a 3^{rd} order polynomial and then subtracted from the uv data.

To calculate the cleaning threshold a dirty image of an emission free channel at 1415.556 MHz was generated with an image size 4096 by 4096 pixels and a robust weighting of 1 and a cell size of 3 arc seconds. 128 w-projection planes were used. The 4th of March observation used the 57 antennas and the resulting beam size 24.46 by 22.00 arc-seconds while the 10th of April observation used the 60 antennas and the resulting beam size 22.73 by 19.47 arc-seconds. The rms noise found for the dirty image in a non-emission channel was 1.604 mJy and 1.565 mJy respectively.

In the 4 of March narrow band observation, the noise for a single outlining field, $M83_6$, the naturally weighted noise was 1.712 mJy. This is about 15% higher than the theoretical rms noise that is expected for $T_{sys}/\eta = 19.7$K, a detailed report on the measurement of the T_{sys}/η for all the antennas in the array is currently in preparation. The 10th of April's observation had a noise of 1.691 mJy for the same field which is about 13% higher than the theoretical rms noise that is expected for $T_{sys}/\eta = 19.7$K.

The naturally weighted noise in the image produced could be improved by using more sophisticated calibration methods e.g. self calibration but these methods would obscure telescope and correlator errors through the calibration. The noise level in the produced image is not an immediate concern as it is reasonably close to the theoretical values considering the minimal calibration and processing done on the data.

The final image, a mosaic of the 7 fields centred on $M83_4$, was then deconvolved down to a threshold of 3 times the rms of the dirty image. 640 channels were imaged from between 1415.55 to 1419.73 MHz which covered the HI emission of M83. CASA's task tclean was used with a Briggs weighting of 1 and a MeerKAT primary beam model of a projected cosine, listed in Appendix A, to do a joint deconvolution of the seven fields of the mosaic and correction for the primary beams sensitivity. This produced a cube of 640 channels with 4096 by 4096 pixels, and a resolution of 24.46 by 22.00 arc seconds for the 4th of March observation and 22.73 by 19.47 for the 10th of April's observation.

This was then passed through the source finding application SoFiA, to extract the neutral Hydrogen and produce the smaller cubes with only the HI emission for each of the detected sources and other diagnostic plots. Further details on the source find process can be found in (Serra et al. 2015), and (Westmeier et al. 2021).

5.1 Bugs

List of bugs encountered.

- CASA can't image 300+ channels in spectral line mode without using more than 500GB of RAM.
- A bug was fixed in the correlator between the two observations, this was a channel labelling issue where the channels would be one channel off.

6 Future plans

We need to redo the imaging process after averaging 8 channels together to allow comparison with wide band fine data. In the future we plan to redo this analysis using the SDP spectral imaging pipeline products and processing.

7 List of references

Barnes et al. 2001, Monthly Notices of the Royal Astronomy Society, 322, 486-498
Heald et al. 2016, Monthly Notices of the Royal Astronomy Society, 462, 1238-1255
Koribalski 2018, Monthly Notices of the Royal Astronomy Society, 478, 1611
Park et al. 2001, Astronomical Society of the Pacific Conference Series, 230, 109-110
Serra et al. 2015, Monthly Notices of the Royal Astronomy Society, 448, 1922
Walter et al. 2008, The Astrophysical Journal, 136,2563-2647
Westmeier et al. 2021, Monthly Notices of the Royal Astronomy Society, 506, 3962

A Supplementary Code

The beam model described below is accurate to about $\approx 5\%$ across the array and over the L-band bandwidth, within the first null of the beam. [1]

```
def beam(offsetx, offsety, freq):
    """freq in MHz
    offsetx, offsety in degrees"""
    FWHM = np.sqrt(89.5*86.2)/60.*(1e3/freq)
    theta = np.sqrt(offsetx**2+offsety**2)
    a = (np.cos(1.189*np.pi*(theta/FWHM))/(1-4*(1.189*(theta/FWHM))**2))**2
    return a

MEERKAT_PB = vp.setpbnumeric(
    telescope='OTHER',
    othertelescope='MeerKAT',
    dopb=True,
    vect=beam(np.linspace(0,3.0,1000),0,1400.0),
    maxrad='3.0deg',
    reffreq='1.4GHz',
    isthispb='PB',
    dosquint=False)

vp.saveastable('MEERKAT_PB.tab')
```

[1] Careful attention needs to be paid to the output logs, as CASA will replace the primary beam model with a different beam model if the imaging mode doesn't support the model type.

M83_mosaic_in_Narrow_bandv2

Final Audit Report 2022-03-14

Created:	2022-03-14
By:	Carmen Humphreys (carmen@ska.ac.za)
Status:	Signed
Transaction ID:	CBJCHBCAABAAO-Dr_2na_JkhLPi2QyG0V3QyPNgvaJzn

"M83_mosaic_in_Narrow_bandv2" History

Document created by Carmen Humphreys (carmen@ska.ac.za)

2022-03-14 - 12:51:02 PM GMT- IP address: 105.225.78.56

Document emailed to Sean Passmoor (sean@sarao.ac.za) for signature

2022-03-14 - 1:05:57 PM GMT

Email viewed by Sean Passmoor (sean@sarao.ac.za)

2022-03-14 - 1:33:34 PM GMT- IP address: 196.24.39.242

Document e-signed by Sean Passmoor (sean@sarao.ac.za)

Signature Date: 2022-03-14 - 1:36:43 PM GMT - Time Source: server- IP address: 196.24.39.242

Document emailed to Sharmila Goedhart (sharmila@sarao.ac.za) for signature

2022-03-14 - 1:36:47 PM GMT

Email viewed by Sharmila Goedhart (sharmila@sarao.ac.za)

2022-03-14 - 1:40:10 PM GMT- IP address: 66.249.93.143

Document e-signed by Sharmila Goedhart (sharmila@sarao.ac.za)

Signature Date: 2022-03-14 - 1:40:48 PM GMT - Time Source: server- IP address: 169.0.109.228

Agreement completed.

2022-03-14 - 1:40:48 PM GMT